Orthogonal control of the frequency comb dynamics of a mode-locked laser diode

Kevin W. Holman, David J. Jones, and Jun Ye

JILA, National Institute of Standards and Technology and University of Colorado, Boulder, Colorado 80309-0440

Erich P. Ippen

Research Laboratory of Electronics, Massachusetts Institute of Technology, Cambridge, Massachusetts 02139

We have performed detailed studies on the dynamics of a frequency comb produced by a mode-locked laser diode (MLLD). Orthogonal control of the pulse repetition rate and the pulse-to-pulse carrier-envelope phase slippage is achieved by appropriate combinations of the respective error signals to actuate the diode injection current and the saturable absorber bias voltage. Phase coherence is established between the MLLD at 1550 nm and a 775-nm mode-locked Ti:sapphire laser working as part of an optical atomic clock. © 2003 Optical Society of America
    OCIS codes: 320.7160, 120.3930, 140.5960.

Optical frequency combs have had major effects on frequency metrology and ultrafast optics.[1–3] A logical next step is to extend the spectral coverage into the 1.5-μm-wavelength region,[4] where a mode-locked laser diode (MLLD) provides a compact, reliable, and efficient source of an optical frequency comb, with future applications including dense wavelength-division multiplexed systems, photonic samplers in high-speed analog–digital conversion, and distribution of optical frequency standards over optical fiber networks. Previously we reported tight synchronization of a 1550-nm MLLD to a Ti:sapphire-based femtosecond (fs) frequency comb that is used as clockwork for an optical atomic clock.[5] In this Letter we explore in detail the dynamics of the frequency comb generated by the MLLD and achieve simultaneous and orthogonal control of the pulse repetition rate and carrier-envelope phase. We have now phase locked the optical carriers of the MLLD and the Ti:sapphire laser.

A phase-coherent link between mode-locked lasers requires two distinct conditions to be met.[6] The comb spacing of the 1550-nm source ($f_{\rm rep,1550}$) must be locked to the optical clock's fs comb spacing ($f_{\rm rep,775}$). Second, the combs' offset frequencies ($f_{\rm ceo,775}$ and $f_{\rm ceo,1550}$) must also be phase locked together. This latter step requires spectral overlap between the two combs. The ultrawide-bandwidth optical frequency comb generated by a mode-locked femtosecond Ti:sapphire laser is phase locked to a highly stable, iodine-based optical frequency standard.[7] The optical comb of the MLLD is frequency doubled and compared against the Ti:sapphire comb at a mutually accessible spectral region to generate a heterodyne beat (Fig. 1). Synchronization of the MLLD to the Ti:sapphire laser was reported in Ref. 5, which discusses the use of a high-bandwidth high-gain electronic feedback loop acting on the diode injection current (I_d) to further reduce the residual phase noise between $f_{\rm rep,775}$ and $f_{\rm rep,1550}$. However, we noticed that, once the synchronization loop was activated, the linewidth of

the heterodyne beat signal containing $f_{\rm ceo,1550}$ became substantially broadened, indicating a strong coupling of the injection current to the carrier-envelope offset frequency of the MLLD. Likewise, any attempt to stabilize the heterodyne beat frequency by the use of either the saturable absorber's reverse bias voltage (V_s) or the diode injection current leads to a significant increase in the timing jitter between the two lasers.

In pursuit of simultaneous synchronization and phase locking, we need to understand the dependence of the MLLD comb dynamics on all the relevant variables, i.e., I_d, V_s, and the corrections (l_c) to the external cavity length, provided by a piezo-activated external cavity mirror. When the value of V_s is increased, the bandgap of the saturable absorber shifts to lower energy, resulting in a larger value of refractive index n at the operating wavelength. A smaller bandgap also leads to an increase in the band-edge curvature, and so $(\mathrm{d}n/\mathrm{d}\omega)$ increases. Hence, the pulse group velocity decreases, leading to a reduced value of $f_{\rm rep,1550}$. This is confirmed by the experimental data, as shown by the circles in Fig. 2(a).
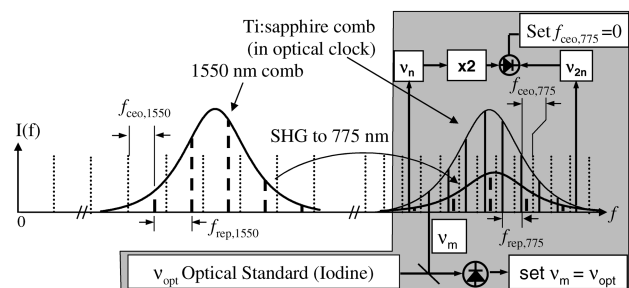

Fig. 1. Schematic diagram of simultaneous synchronization and phase locking between a 1.55-μm MLLD and a 775-nm mode-locked Ti:sapphire laser. The shaded area shows the implementation of an optical clock based on a Ti:sapphire fs comb phase-stabilized to an iodine standard. The MLLD's repetition frequency is eight times that of the Ti:sapphire (not as shown in the figure).
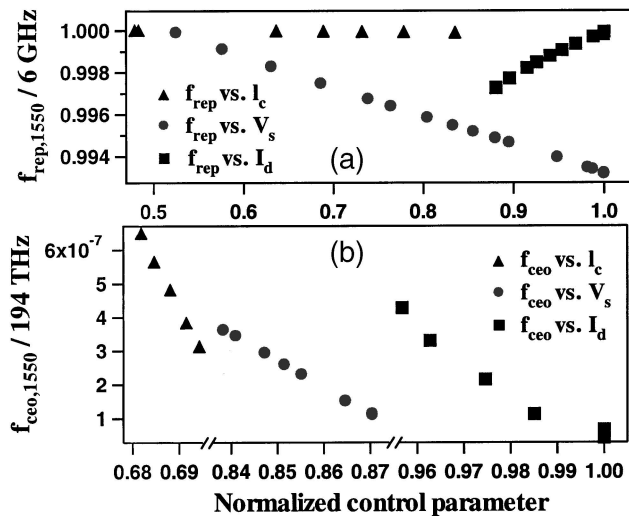
Fig. 2. Dependence of $f_{rep,1550}$ and $f_{ceo,1550}$ on I_d, V_s, and l_c. All three parameters have been normalized by their maximum operating value. When $f_{rep,1550}$ was evaluated, the rf injection was turned off to observe the uncontaminated response to I_d, V_s, and l_c.

The differential rates of change of n and $(dn/d\omega)$ also cause a change in $f_{ceo,1550}$ as V_s increases, as shown by the circles in Fig. 2(b). Determination of the changes in $f_{rep,1550}$ and $f_{ceo,1550}$ reveals the dependence of n and $(dn/d\omega)$ on V_s.[8] On the other hand, when I_d increases, the enhanced free-carrier density leads to smaller values of n and hence larger values of $f_{rep,1550}$, confirmed by data in the squares in Fig. 2(a). Again, measurement of $f_{rep,1550}$, coupled with that of $f_{ceo,1550}$ versus I_d, determines both n and $(dn/d\omega)$ versus I_d. The influence of I_d on $(dn/d\omega)$ is more complicated and is related to the wavelength and the current dependence of the linewidth enhancement factor (α) of the specific diode structure. Experimentally we find that larger I_d leads to smaller $f_{ceo,1550}$, as shown by the data in the squares in Fig. 2(b).

Figure 2 summarizes that changes in V_s affect both $f_{ceo,1550}$ and $f_{rep,1550}$ in a similar manner, while changes in I_d cause opposite changes in $f_{ceo,1550}$ and $f_{rep,1550}$. Of course, changes in l_c also affect both $f_{ceo,1550}$ and $f_{rep,1550}$. The magnitude of the effect that l_c has on $f_{ceo,1550}$ is comparable to that caused by I_d or V_s, if a similar amount of fractional change in the control parameters is involved. However, the effect of l_c on $f_{rep,1550}$ is negligibly small compared with that caused by similar fractional changes in I_d and V_s. We can hence improvise the following strategy for optimal control. Clearly, error signals associated with fluctuations of both $f_{ceo,1550}$ and $f_{rep,1550}$ need to be combined linearly with appropriate signs and gains, respectively, to produce two control signals, one for I_d and the other for V_s. This process represents a simple diagonalization of a 2×2 matrix, leading to two orthogonal control loops for $f_{ceo,1550}$ and $f_{rep,1550}$. In addition, the piezo-activated external cavity mirror can be used to vary l_c so that a higher loop gain in the low-frequency range can be implemented to control $f_{ceo,1550}$. As noted, sensitivity of the l_c change on

$f_{rep,1550}$ is small and hence can be neglected in the orthogonalization of the control loop.

With the implementation of the orthogonal control loop, we can achieve simultaneous stabilization of $f_{ceo,1550}$ and $f_{rep,1550}$ with basically no compromise in performance for either $f_{ceo,1550}$ or $f_{rep,1550}$ compared with the optimized single-parameter control for either variable independently. The MLLD repetition rate $f_{rep,1550}$ is first stabilized to $f_{rep,775}$ by modulation of the saturable absorber with an injection microwave signal that is extracted from the iodine-based optical atomic clock. We note that, as the injection power to the saturable absorber is increased, the stability of $f_{rep,1550}$ is enhanced, but the stability of $f_{ceo,1550}$ decreases dramatically. For the same reason that an orthogonal feedback control is implemented within the loop bandwidth, the microwave injection signal should be simultaneously fed into the saturable absorber and the laser diode injection current with proper phases and amplitudes such that the synchronization's undesired side effect on $f_{ceo,1550}$ can be minimized. This observation is important for future designs of MLLDs where high-frequency (6 GHz for the current MLLD) modulation capability should be accommodated for both the saturable absorber and the injection current. The synchronization error signal[5] is fed into the orthogonal control loop. To phase lock the MLLD's $f_{ceo,1550}$ to that of the optical clock, the optical output of the MLLD is first amplified by two stages of erbium-doped fiber amplifiers and then focused into a 2-cm-long piece of periodically poled lithium niobate for efficient second-harmonic generation, producing 35 μW centered at 775 nm. The frequency-doubled signal from the MLLD is then collinearly combined with the Ti:sapphire femtosecond comb to generate a heterodyne beat ($= 2f_{ceo,1550} - f_{ceo,775}$). The heterodyne beat is processed by a digital phase detector against a stable radio-frequency reference, and the subsequent error signal is fed into the orthogonal control loop.

Figure 3 demonstrates the effect of the orthogonal control loop optimized for both $f_{ceo,1550}$ and $f_{rep,1550}$. The dashed line represents the spectral density of the
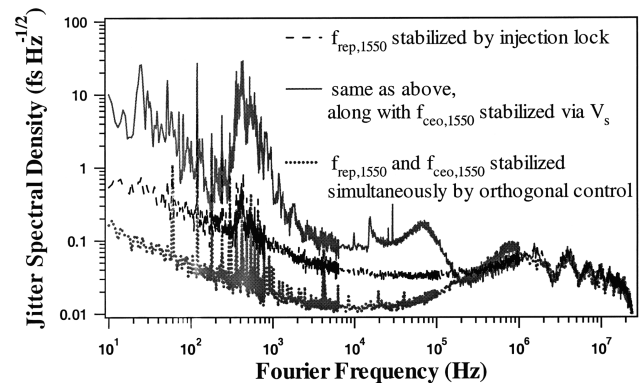

Fig. 3. Relative timing jitter for the synchronization loop under the conditions of (a) microwave injection to the saturable absorber (dashed trace), (b) synchronization via injection locking and phase locking via saturable absorber bias voltage (solid trace), and (c) synchronization and phase locking via orthogonalized control (dotted trace).
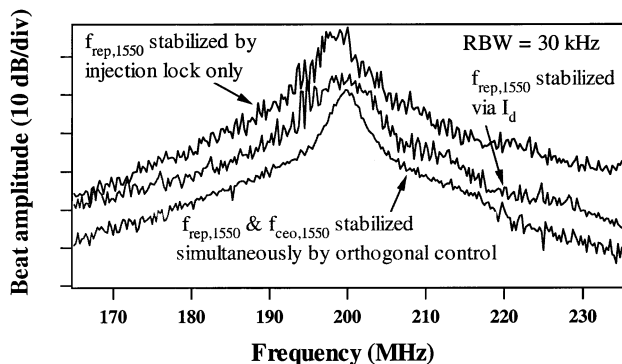
Fig. 4. Heterodyne beat signal between the frequency-doubled MLLD and the Ti:sapphire combs under the conditions of (a) synchronization via microwave injection to the saturable absorber (top trace), (b) synchronization via injection current (I_d) servo (middle trace), and (c) synchronization and phase locking via orthogonalized control (bottom trace). Traces are vertically displaced for viewing clarity.
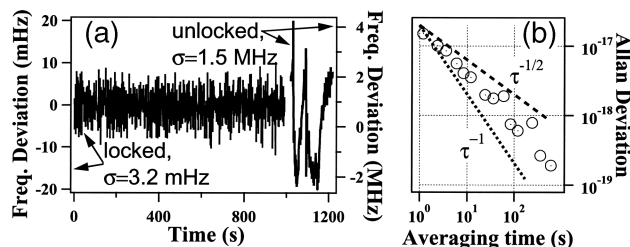

Fig. 5. (a) Heterodyne beat recorded by a frequency counter at 1-s gate time, under no phase locking (short trace, with respect to the right vertical axis) and phase locking (long trace, with respect to the left vertical axis). (b) Allan deviation associated with the phase-locked signal.

residual timing jitter obtained by comparison of the phase of $f_{\mathrm{rep},1550}$ against that of ($8 \times f_{\mathrm{rep},775}$) when the lasers are synchronized by injection of the external microwave clock signal to the saturable absorber. Any attempt to stabilize $f_{\mathrm{ceo},1550}$ by control of V_s leads to increased timing jitter in the synchronization loop, as shown by the solid trace in Fig. 3. However, by maintaining the microwave injection to the saturable absorber and activating the orthogonal control loop to stabilize both $f_{\mathrm{ceo},1550}$ and $f_{\mathrm{rep},1550}$, we can further reduce the residual timing jitter within the bandwidth of the servo loop, shown by the dotted trace in Fig. 3. This level of performance for the synchronization loop is basically the same as if only $f_{\mathrm{rep},1550}$ is stabilized while $f_{\mathrm{ceo},1550}$ is left floating.

Figure 4 illustrates the second important aspect of the orthogonal control. Three traces are shown in the figure, depicting the line shape of the heterodyne beat signal ($2f_{\mathrm{ceo},1550} - f_{\mathrm{ceo},775}$) under three different experimental conditions. The top trace represents the beat signal when the MLLD is synchronized to the Ti:sapphire laser via injection to the saturable absorber. When the synchronization is further improved by closure of a feedback loop using I_d, indeed, the phase error (corresponding to the residual timing

jitter) of the $f_{\mathrm{rep},1550}$ loop is reduced. However, the linewidth of the heterodyne beat, and hence $f_{\mathrm{ceo},1550}$, is broadened, as shown by the middle trace in Fig. 4. Again, when the orthogonal control loop is activated, not only is the $f_{\mathrm{rep},1550}$ loop improved as shown in Fig. 3, but the coherence of $f_{\mathrm{ceo},1550}$ is also improved as shown by the narrowed line shape of the bottom trace in Fig. 4.

Figure 5(a) shows frequency-counting records of the beat between the MLLD and Ti:sapphire combs under locked and unlocked conditions. At 1-s gate time, the rms fluctuation (σ_{rms}) of the heterodyne beat is 1.5 MHz when $f_{\mathrm{ceo},1550}$ is not stabilized. Under the orthogonal control condition, σ_{rms} of ($2f_{\mathrm{ceo},1550} - f_{\mathrm{ceo},775}$) is reduced to 3.2 mHz. By monitoring the beat error signal produced by the digital phase detector we ensure that no cycles have slipped over this measurement period. Allan deviation[9] of the stabilized beat frequency record is shown in Fig. 5(b), determined with respect to the 1550-nm optical carrier frequency. The deviation averages down somewhere between $1/\tau$ and $1/\sqrt{\tau}$ (τ is the averaging time), indicating a mixture of white frequency and phase noise in our phase-locked loop.

In summary, we have presented a complete characterization of the comb dynamics of a mode-locked laser diode. The study has led to a successful implementation of an orthogonal feedback control that simultaneously stabilizes the repetition rate and the carrier-envelope offset frequency of the MLLD. Optical coherence between the 1550- and 775-nm combs has been established, with further improvement possible by use of a better design of the MLLD system.

References

1. D. J. Jones, S. A. Diddams, J. K. Ranka, A. Stentz, R. S. Windeler, J. L. Hall, and S. T. Cundiff, Science **288,** 635 (2000).
2. Th. Udem, R. Holzwarth, and T. W. Hänsch, Nature **416,** 233 (2002).
3. A. Baltuska, Th. Udem, M. Uiberacker, M. Hentschel, E. Goulielmakis, Ch. Gohle, R. Holzwarth, V. S. Yakovlev, A. Scrinzi, T. W. Hänsch, and F. Krausz, Nature **421,** 611 (2003).
4. F. Tauser, A. Leitenstorfer, and W. Zinth, Opt. Express **11,** 594 (2003), http://www.opticsexpress.org.
5. D. J. Jones, K. W. Holman, M. Notcutt, J. Ye, J. Chandalia, L. A. Jiang, E. P. Ippen, and H. Yokoyama, Opt. Lett. **28,** 813 (2003).
6. R. K. Shelton, L.-S. Ma, H. C. Kapteyn, M. M. Murnane, J. L. Hall, and J. Ye, Science **293,** 1286 (2001).
7. J. Ye, L.-S. Ma, and J. L. Hall, Phys. Rev. Lett. **87,** 270801 (2001).
8. K. W. Holman, R. J. Jones, A. Marian, S. T. Cundiff, and J. Ye, Opt. Lett. **28,** 851 (2003).
9. D. W. Allan, Proc. IEEE **54,** 221 (1966).